2019

Multiplexed detection of autoantibodies for Type 1 Diabetes using nanopore thin-film based sensors

Subin Mao
Iowa State University

Multiplexed detection of autoantibodies for Type 1 Diabetes using nanopore thin-film based sensors

by

Subin Mao

A thesis submitted to the graduate faculty

in partial fulfillment of the requirements for the degree of

MASTER OF SCIENCE

Major: Electrical Engineering

Program of Study Committee:
Long Que, Major Professor
Jiming Song
Ian Schneider

The student author, whose presentation of the scholarship herein was approved by the program of study committee, is solely responsible for the content of this thesis. The Graduate College will ensure this thesis is globally accessible and will not permit alterations after a degree is conferred.

Iowa State University

Ames, Iowa

2019

DEDICATION

I would like to dedicate this thesis to my parents Pinggui Mao and Yulian Zhang. I would not be able to complete this work without their unreserved love and financial support.

I would like to dedicate this thesis to my major professor, Dr. Long Que. I would not complete this work without his guidance.

I would like to dedicate this thesis to my friends who stay with me in the past two years.

TABLE OF CONTENTS

Page

LIST OF FIGURES v

NOMENCLATURE vii

ACKNOWLEDGMENTS viii

ABSTRACT ix

CHAPTER 1. GENERAL INTRODUCTION 1
1.1 Research Motivation 1
1.2 Thesis Organization 3
References 4

CHAPTER 2. DETECTION OF AUTOANTIBODIES FOR TYPE 1 DIABETES USING LABEL-FREE OPTICAL SENSOR 5
Abstract 5
2.1 Introduction 5
2.2 Principle of Optical Sensor 8
2.3 Experimental Procedures 9
2.4 Results and Discussion 12
References 17

CHAPTER 3. FABRICATION OF LABEL-FREE OPTICAL SENSOR WITH MICROFLUIDICS INTERFACE 20
Abstract 20
3.1 Introduction 20
3.2 Materials and Fabrication process 23
1. Materials and chemicals 23
2. Micropattern AAO process 23
3.3 Results and Discussion 27
1. Fabricated Device 27
2. Microfluidic Operation Demonstration 28
3. Measurements and Data Analysis 29
References 30

CHAPTER 4. CONCLUSION 31

APPENDIX A. ANODIC ALUMINUM OXIDE FORMATION MECHANISM 32
Reference 34

APPENDIX B. SURFACE FUNCTIONALIZATION MATERIALS AND PROTOCOL 35
Material 35
Protocol 36

APPENDIX C.THE OPERATIONAL PRINCIPLE OF ANODIC ALUMINUM OXIDE 38
References 40

LIST OF FIGURES

Fig 2. 1 (a) structure of the Anodic Aluminum Oxide, arrays of uniform and parallel nanopores. (b) SEM image of AAO showing the nanopores of the sensor 8

Fig 2. 2 Operational principle of sensor: when antigen (Ag) is bound to antibody (Ab), the fringes of the reflected optical signal shift 9

Fig 2. 3 Demonstration of the step by step surface functionalization process 11

Fig 2. 4 (a) Typical measured optical signal for GAD Ab at 0, 15 mins and 30 mins incubation time, fringes shift as the incubation time increased until saturated. (b) Measurement of insulin Ab with different concentration, 0, 0.4 U/ml, and 12.5 U/ml, the higher insulin Ab concnetration, the larger fringes shift. 12

Fig 2. 5 (a) Insulin Ab saturation time around 30 to 45 mins (b) GAD Ab saturation time around 30 to 45 mins (c) IA-2 Ab saturation time around 30 to 45 mins 13

Fig 2. 6 (a) Standard test of Insulin antibody as concentration from 0.01 U/ml to 50 U/ml in both serum and buffer. (b) Standard test of GAD antibody from 0.01 U/ml to 50 U/ml only in serum. (c) Standard test of IA-2 antibody from 0.01 U/ml to 100 U/ml only in serum. Note that concentrations of the anti-insulin in buffer are known provide by vendor (adi Inc), as well as the concentration of antibodies against GAD, IA-2 in serum are known provided by Kronus. 14

Fig 2. 7 (a) Specificity test of insulin antigens functionalized with three antibodies. (b) Specificity test of GAD antigen functionalized with three antibodies (c) Specificity test of IA-2 antigen functionalized with three antibodies. 16

Fig 3. 1 Fabrication flow of micropattern AAO thin film sensor 25

Fig 3. 2 Photomask of micropattern AAO nanopore thin film with the diameter of 3.5 mm 25

Fig 3. 3 SketchUp designed photomask for optical sensor. 26

Fig 3. 4 Cross-section view of photolithographt and PDMS soft lithography process 27

Fig 3. 5 Schematic of a device containing 3-row nanopore thin-film based sensors 28

Fig 3. 6 (a) photo of a fabricated device containing 3-row nanopore thin-film based sensors; (b) SEM image showing the nanopores of the sensor. 28

Fig 3. 7 Photo of the device: three food dyes (blue, red and green) to mimic three autoantibodies inside the chip showing its capability for multiplexed detection of three autoantibodies (insulin Ab, GAD Ab, and IA-2 Ab) by three sensors in three rows. 29

Fig A. 1 Experimental Equipment for producing anodic aluminum oxide [1] 33

Fig A. 2 (a) Schematic of the major features involved in the formation of the barrier layer. (b) Schematic of pore formation mechanism in an acidic electrolyte [1] 34

Fig C. 1 Schematic of the label-free nanostructured uFPI biosensor: Au-coated nanostructures are embedded in the FPI cavity [2][3] 39

Fig C. 2 (a) Immoblization of antigen on the side wall of the nanopore, and after binding with antibody. (b) fringes indicate the signal produced from receptor only and after binding with antibody, fringes shift $\Delta\lambda$ on the change of the effective refractive index. 39

NOMENCLATURE

T1D	Type 1 Diabetes
GAD	Glutamic Acid Decarboxylase
IA-2	Insulinoma associated Protein-2
ELISA	Enzyme-Link Immunosorbent Assay
RIA	Radioimmunoassay
AAO	Anodic Aluminum Oxide

ACKNOWLEDGMENTS

I would like to thank my committee chair, Long Que, and my committee members Jiming Song and Ian Schneider, for their guidance and support throughout the course of this research.

I would like to thank our group members, Chao Song, Silu Feng, Renyuan Yang and Xiaoke Ding for their valuable research experience and support.

In addition, I would also like to thank my friends, the department faculty and staff for making my time at Iowa State University a wonderful experience. I want to also offer my appreciation to those who were willing to participate in my surveys and observations, without whom, this thesis would not have been possible.

ABSTRACT

This thesis reports on using label-free optical sensors for multiplexed detection of autoantibodies for Type 1 Diabetes. An autoimmune disease that occurs when the body either does not produce enough or stops producing insulin, the hormone that controls blood-sugar levels. Autoantibodies working against islet antigens such as insulin, glutamic acid decarboxylase (GAD), and insulinoma associated protein-2 (IA-2) have been well-confirmed in Type 1 Diabetes (T1D) panels. While clinical diagnosis of T1D can be performed by detecting the level of autoantibodies in a blood sample, sensitive detections are especially crucial for predictive analysis and early screening of potential diabetes victims.

The label-free optical sensor was made from Anodic Aluminum Oxide (AAO), a self-organized material formed by high-density arrays of uniform and parallel porous nanostructures, which has been widely utilized in biomedical sensing and bioanalysis area. We have demonstrated multiplexed detection of autoantibodies using label-free optical sensors that can readily detect as a small level as 0.1 U/ml of three autoantibodies in human serum. In addition, the specificity of the sensor has also been evaluated by detecting autoantibodies in a nonspecific antigen with results reflecting good specificity. Moreover, multiplexed detection of insulin, GAD, and IA-2 antibodies in serum using such chip has also been demonstrated.

CHAPTER 1. GENERAL INTRODUCTION

1.1 Research Motivation

Diabetes is a chronic disease that occurs either when the human pancreas does not produce enough insulin, or the body ineffectively uses the insulin it does produce. Insulin is a type of hormone that takes control of the blood-sugar levels within a reasonable range. Hyperglycemia or high blood sugar, a common side effect of diabetes, can trigger havoc on organs, especially blood vessels, kidneys, and the nerve system, elevating the risk of heart attack and stroke over time.

There are two main kinds of diabetes, Type 1 and Type 2. Type 1 diabetes, also known as insulin-dependent or juvenile diabetes, is an autoimmune disease, characterized by deficiency in production of insulin, caused by the immune system attacking itself, with the body attacking the insulin-producing beta cell (islet cell). [1] Over time, the number of islet cells could be tremendously reduced until none remain in the body, so body cannot produce its own insulin, resulting in disuse of glucose in bloodstream, i.e., without insulin, the body cannot obtain energy from blood glucose. Type 1 Diabetes is neither preventable nor curable, is of uncertain cause, and requires lifelong treatment once developed, while Type 2 Diabetes is preventable and sometimes it can be reversed. The pathogenesis of Type 2 Diabetes is the body's improper use of insulin and body resist the insulin [1], with free fatty acids promoting loss of insulin sensitivity in such a case.[2] The majority of people with diabetes have Type 2 Diabetes, and the main reasons for T2D are obesity and lack of physical exercise.[3]

According to World Health Organization (WHO) statistics, the number of people with diabetes has risen from 108 million in 1980 to 440 million in 2014, and around the world

rates of incidence of Type 1 Diabetes are rising; in the United States, approximately 1.25 million American have Type 1 diabetes and by 2050, 5 million people are expected to be diagnosed with that disease. While it is usually diagnosed in children, youth, but it can develop at any age. Between 2011 and 2012, approximately 17,900 children and juvenile under the age of 20 have been diagnosed with Type 1 Diabetes, and the likelihood. Of being diagnosed with T1D under the age of 20 is still increasing. By 2050, 600,000 people under the age of 20 are expected to be diagnosed as having Type 1 Diabetes. [4] [5]

TrailNet, an NIH-funded international network of research centers, claimed that diagnosing Type 1 Diabetes as early as possible before beta cells (islet cells) completely disappear is important in reducing the risk of T1D. [6] For most people with T1D, the disease seems to take place suddenly, often accompanied by severe symptoms. Research studies state that Type 1 Diabetes can be divided into three different stages. Stage 1 occurs at the beginning of the T1D, with individuals testing positive for two or more autoantibodies, indicating the immune system has begun attacking beta cells, although at this stage, the blood-sugar level within a normal range. Advancing to stage 2, in which a victim tests positive for two or more diabetes-related autoantibodies, blood-sugar levels become abnormal and the beta cell damage continues. At stage 3, T1D can be clinically diagnosed by recognition of a great loss of beta cells, and other common symptoms of T1D. Earlier diagnosis is therefore extremely important to either reduce the risk of having T1D or trigger its satisfactory management by intervening with loss of the beta cell during the early T1D stage. However, because of testing expense, people tend not participate in early screening if they have no symptoms of Type 1 Diabetes.

Because of the increased number of people under age 20 who are suffering from the torment of Type 1 Diabetes, I have introduced a method for rapid detection of the three main autoantibodies for Type 1 Diabetes using a label-free optical sensor based on Anodic Aluminum Oxide (AAO) substrate suitable for bioanalysis.

In this thesis, some of current state-of-the-art with detection of autoantibodies will be discussed, along with details of experiment procedures, fabrication process, and results.

1.2 Thesis Organization

The following chapters focus mainly on experimental details, including the sensor's operating principle, experiment process, experimental results and fabrication flow of sensor. Chapter 2 discusses the operational principles of the Anodic Aluminum Oxide (AAO)-based thin film sensor, experimental procedures, and discussion of study's results, that describe sensor sensitivity to change in concentration of autoantibodies. Furthermore, it will also describe further experiments related to specificity test, in which detection of the autoantibodies related to nonspecific antigen was used to evaluate the sensor's specificity with good results.

Chapter 3 will demonstrate the details of label-free optical sensor integrated on chip fabrication flow and will describe the procedures whereby a microfluidic interface and AAO based optical sensor integrated onto a chip. Additional applications of this sensor will also be discussed. Appendix A describes the mechanism of anodic aluminum oxide formation. [7] Appendix B provides the protocol of the surface functionalization process and describes the

materials used in the experiment. Appendix C provides detailed information regarding the operational principles of the label-free optical sensor. [8]

References

[1] American Diabetes Association. (2010). Diagnosis and classification of diabetes mellitus. *Diabetes care*, *33*(Supplement 1), S62-S69.

[2] Saini, V. (2010). Molecular mechanisms of insulin resistance in type 2 diabetes mellitus. *World journal of diabetes*, *1*(3), 68.

[3] World Health Organization. (1999). *Definition, diagnosis and classification of diabetes mellitus and its complications: report of a WHO consultation. Part 1, Diagnosis and classification of diabetes mellitus* (No. WHO/NCD/NCS/99.2). Geneva: World health organization.

[4] World Health Organization. (2016). Global report on diabetes.

[5] Centers for Disease Control and Prevention. (2017). National diabetes statistics report, 2017.

[6] Benson, D., & Benson, D. (2016, February 22). Type 1 diabetes new staging system promotes early detection. Retrieved from https://www.bcm.edu/news/diabetes/type-1-diabetes-early-detection.

[7] He, Y., Li, X., & Que, L. (2012). Fabrication and characterization of lithographically patterned and optically transparent anodic aluminum oxide (AAO) nanostructure thin film. *Journal of nanoscience and nanotechnology*, *12*(10), 7915-7921.

[8] Zhang, T., Gong, Z., Giorno, R., & Que, L. (2010). A nanostructured Fabry-Perot interferometer. *Optics express*, *18*(19), 20282-20288.

CHAPTER 2. DETECTION OF AUTOANTIBODIES FOR TYPE 1 DIABETES USING LABEL-FREE OPTICAL SENSOR

Abstract

Anodic Aluminum Oxide (AAO) was discovered almost a century ago and has been widely utilized. It has a honeycomb-like nanostructure characterized by arrays of uniform and parallel porous nanostructures. AAO has been considered as a promising nanomaterial for developing biosensing systems with remarkable performance, and recent studies have demonstrated use of AAO with other techniques, yielding numerous state-of-the-art sensors for use in bioanalysis and other applications. Beta cell (islet cell) autoantibodies such as insulin, glutamic decarboxylase (GAD), and insulinoma associated protein-2 (IA-2) are strongly related to the development of Type 1 Diabetes, and this chapter indicates the sensitive detection of concentration changes in these three autoantibodies on a surface functionalized Anodic Aluminum Oxide surface.

2.1 Introduction

Diabetes is a condition in which a high concentration of sugar or glucose exists in the bloodstream because either the body lacks insulin or doesn't use insulin properly by not converting the sugar to energy. While the majority of diabetes cases occur because the body use insulin inappropriately, about 5% to 10% diabetes caused by lack of insulin, a condition called Type 1 Diabetes. [1]

Although such deficiencies accounts for only a minority of diabetes cases, it maintains a severe chronic disease, usually developing at an earlier age than Type 2 Diabetes, and there is presently a significant trend toward its occurrence at decreasing age.

Type 1 Diabetes is a disease in which pancreatic islet cell destruction results in loss of insulin with the immune system attacking islet cells for unknown reason leading to the body's inability to produce insulin. Detection of autoantibody levels of Type 1 Diabetes, including insulin, GAD, and IA-2 has been of great interest in exploring the diabetes' pathogenesis. Approximately 66% of patients have tested positive with respect to autoantibody attacks insulin [2], while those against GAD are found in 80% of Type 1 Diabetes patients,[2] 16% of whom are under age of 25. [3] In addition, the presence of antibodies against IA-2 ranges from 54% to 75%. [4] And, more importantly, children have a higher chance to develop Type 1 Diabetes, with the peak age of diagnosis in the United State being about 14 years old. [5] Therefore, earlier diagnosis and predictive screening are particularly urgent in managing Type 1 Diabetes at an early stage for the new generation. Sensitive detection of autoantibodies against beta cell is especially essential for providing T1D predictive value.

Currently, standard detection methods for diabetes autoantibodies use enzyme-link immunosorbent assay (ELISAs) [6] and radioimmunoassay (RIAs) [7]. ELISA is the most commonly used in clinical settings to provide accurate detection and quantification of bio-agents. It is a reliable, sensitive method that requires a strict environment for proper detection to encounter the ELISA. However, ELISA does have obvious shortcomings; it is a labor-intensive, complicated procedure, requires a large volume of sample, and is unable to realize the multiplexed detection. Besides, RIA, that can produce high-specific and high-sensitive results, also has some limitations; it can produce hazard radiation for the user, it's time-consuming, and it is restricted to use of radioactive material. Many approaches have been proposed to seek improved methods for autoantibodies detection, for instance, near-infrared

fluorescence-enhanced detection using a plasmonic gold chip [8], and multiplexed detection using microfluidic droplet array. [9] But there continues to be great need for a simple method of quantitative detection of all three antibodies in a single volume.

For this purpose, we have demonstrated a new method for rapid detection of autoantibodies against insulin, GAD and IA-2 using AAO based optical sensor. The label-free optical sensor is a nanopore-structure-based substrate with a microfluidic interface device. The nanopore structure of such a substrate can utilized Anodic Aluminum Oxide (AAO) to facilitate autoantibody bio-detection. AAO has been discovered and widely used since the early 20th century, is a honeycomb-like structure characterized by arrays of uniform and parallel porous nanostructures, as shown in **Fig 2.1(a)**, with the nanopore diameter size typically ranging from 20nm to 150 nm. A scanning electron microscope (SEM) image of the AAO surface is shown in **Fig 2.1(b)**, and detailed formation mechanism of AAO are given in Appendix A. Because of its incredible performance, there is a great of interest in AAO as a promising nanomaterial for developing bio-detection. Recent studies have demonstrated that AAO can be used in other applications, such as detection of cancer biomarker and Alzheimer's biomarkers [10] [11][14], pressure sensing [12], drug release and loading [13], detection of theophylline [15], detection of Alzheimer's disease [16] and nanostructured optical biosensor [17]. These applications have effectively used AAO along with other techniques to enhance the field of biosensing.

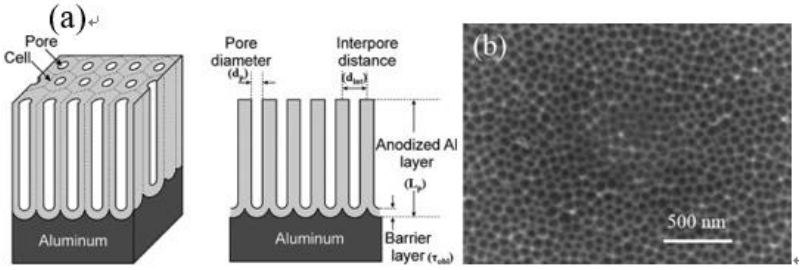

Fig 2. 1 (a) structure of the Anodic Aluminum Oxide, arrays of uniform and parallel nanopores. (b) SEM image of AAO showing the nanopores of the sensor

2.2 Principle of Optical Sensor

The label-free optical sensor uses the nanopore thin film AAO as a platform for facilitating antibody detection. Uniform and parallel nanopores of diameter of typically varying between 20 nm to 150 nm are distributed over the AAO thin film. Each nanopore formed as a cavity can be treated as a nanostructured Fabry-Perot interferometer (μFPI) that can offer advantages, such as increasing sensing surface area, extending penetration depth of incident light, and signal magnification. The operational principle is shown in **Fig 2.2**. When the optical fiber emits a signal on the surface on which there are autoantibodies bound to antigens, the optical signal (fringes) reflected from the sensor will be shifted due to the change in the effective optical thickness at the sensor surface, and this optical shift can be used as a transducing signal.

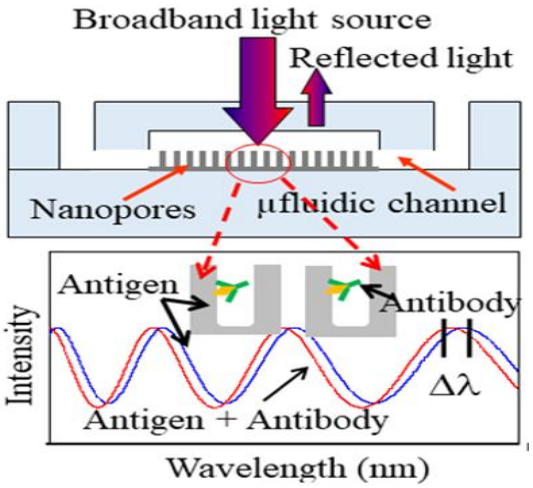

Fig 2. 2 Operational principle of sensor: when antigen (Ag) is bound to antibody (Ab), the fringes of the reflected optical signal shift

2.3 Experimental Procedures

The step-by-step surface functionalization procedure of the sensor is illustrated in **Fig 2.3**. Three different antigens (insulin, GAD, IA-2) are functionalized on the sensor and thereby become capable of detection. More precisely, an AAO slide is prepared by coating it with a thin gold layer using the sputtering apparatus, followed by immereion of the Au-coated AAO sample into a $HSC_{10}COOH/HSC_8OH$ solution, and after incubating overnight at 4°C, the AAO sample is washed with ethanol and deionized (DI) water respectively. After the surface has dried, 200 μL EDC/NHS is applied on the AAO surface and incubating at room temperature for two hours. The sensor surface is then washed with phosphate buffered saline (PBS) and DI water, and after the residual is removed, diabetes antigens are separately applied on the sensor surface and incubated overnight at 4°C. The antigens are then removed by rinsing several times with PBS and DI water, to ensure that no antigens residually remain on the surface, followed by dipping 200 μL EA solution on the surface at room temperature

to block non-occupied site activate by the EDC/NHS solution. After two hours, the AAO surface is rinsed multiple times with PBS and DI water to dispel any leftover EA solution, after which the optical signal (fringes) is recorded. At this point, the surface functionalization procedure has been completely carried out, and the AAO surface is ready to be used in the experiment.

This experiment consists of two parts, incubation-time tests, and standard tests. The incubation time test is to determine how long it takes for the optical signal shift to become stable, while the standard test is to detect whether or not autoantibodies exist on the surface. During the incubation time test, the antigens functionalized AAO sample is immersed in solution containing corresponding antibodies at the highest sample concentration (50 U/ml for insulin antibodies, 50 U/ml, and 100U/ml). Note that the biomarkers of antibody concentrations are provided by the vendor, expressed in the international unit of U/ml. The sensor is shaken on a Shaker for a certain time, followed by cleaning step that includes, repeatedly rinsing the sensor with PBS and DI water, then recording the optical signal. These process, immersing sensor into solution, shaking it, cleaning it, and recording fringes at the specific accumulated time, are then repeated at selected times of 5 mins, 10 mins, 15 mins, 20 mins, 30 mins, 45 mins, 60 mins, and 90 mins. The standard test includes, dipping into a different concentration of biomarker solution with a specific antibody on the antigen functionalized sensor, shaking for 45 mins (the result of the incubation time test), rinsing it with PBS and DI water, and recording the fringes. The concentrations of the antibodies hostile to insulin diluted in the buffer solution are 0 (sample buffer), 0.1 U/ml, 0.1U/ml, 0.4 U/ml, 1.6U/ml, 6.3 U/ml, 12.5 U/ml, 50 U/ml, and the insulin-hostile antibodies diluted in

human serum at the same concentrations. The concentrations of antibody hostile to GAD diluted in human serum are 0 (human serum), 0.1 U/ml, 0.5 U/ml, 1 U/ml, 5 U/ml, 10 U/ml, and 50 U/ml, while the concentrations of antibody against IA-2 diluted in human serum are 0 (human serum), 0.1 U/ml, 1 U/ml, 5 U/ml, 10 U/ml, 50 U/ml and 100 U/ml.

Furthermore, specificity tests were implemented to evaluate the sensors specificity. The sensor was functionalized with antigens then evaluated with other types of antibodies, incubating GAD and IA-2 antibodies on the insulin antigen-functionalized sensor respectively, incubating insulin and GAD antibodies on the IA-2 antigen-functionalized sensor respectively, and incubating insulin and IA-2 antibodies on the GAD antigen-functionalized sensor respectively using the standard processes. A total of 6 sets of tests will be performed. The same antibody concentrations used in standard test were used to implement the specificity test. A small fringe shift can be observed, possibly caused by non-specific binding, since there might be in the serum some unknown compound that can bind with antigens.

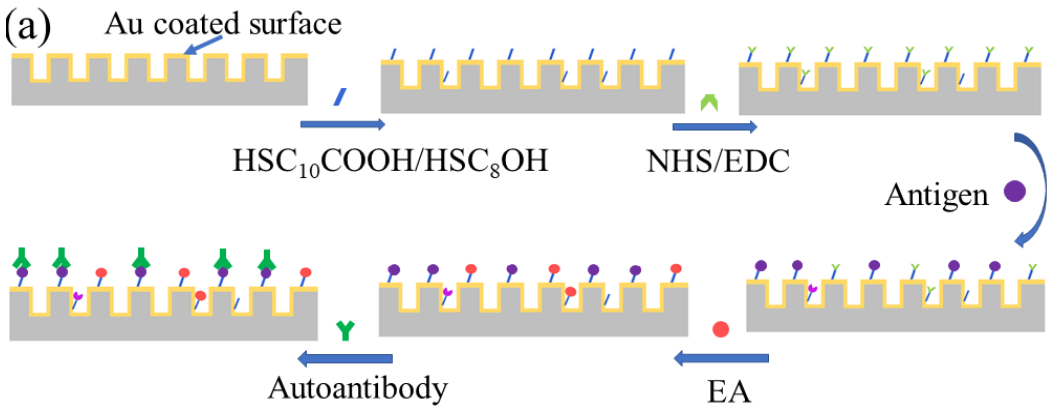

Fig 2. 3 Demonstration of the step by step surface functionalization process

2.4 Results and Discussion

Typically, optical signals from sensor before and after applying the biomarker solution with antibodies will cause a signal shift, as shown in **Fig 2.4**, and the optical shift occurs between two different states of the sensor, at different incubation times, and with different antibody concentrations. In the incubation time test, read the shift between two time-nodes for each sample, until the signal remains unchanged, and calculate the average of each test for three autoantibodies. The incubation time test shows that, all three antibodies need approximately 30 to 45 minutes of incubation time to become saturated. The incubation-time results are shown in **Fig 2.5**.

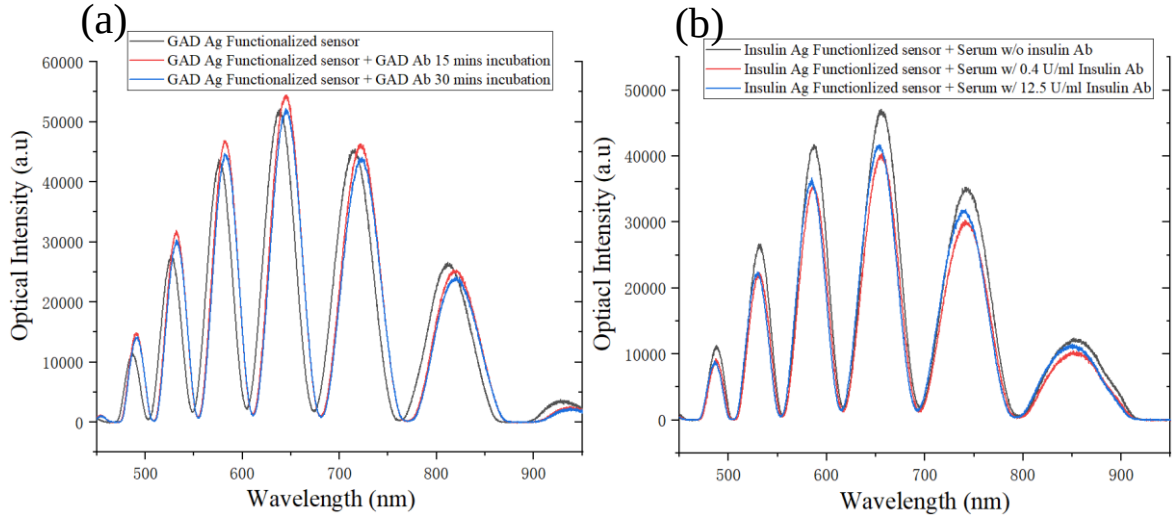

Fig 2. 4 (a) Typical measured optical signal for GAD Ab at 0, 15 mins and 30 mins incubation time, fringes shift as the incubation time increased until saturated. (b) Measurement of insulin Ab with different concentration, 0, 0.4 U/ml, and 12.5 U/ml, the higher insulin Ab concnetration, the larger fringes shift.

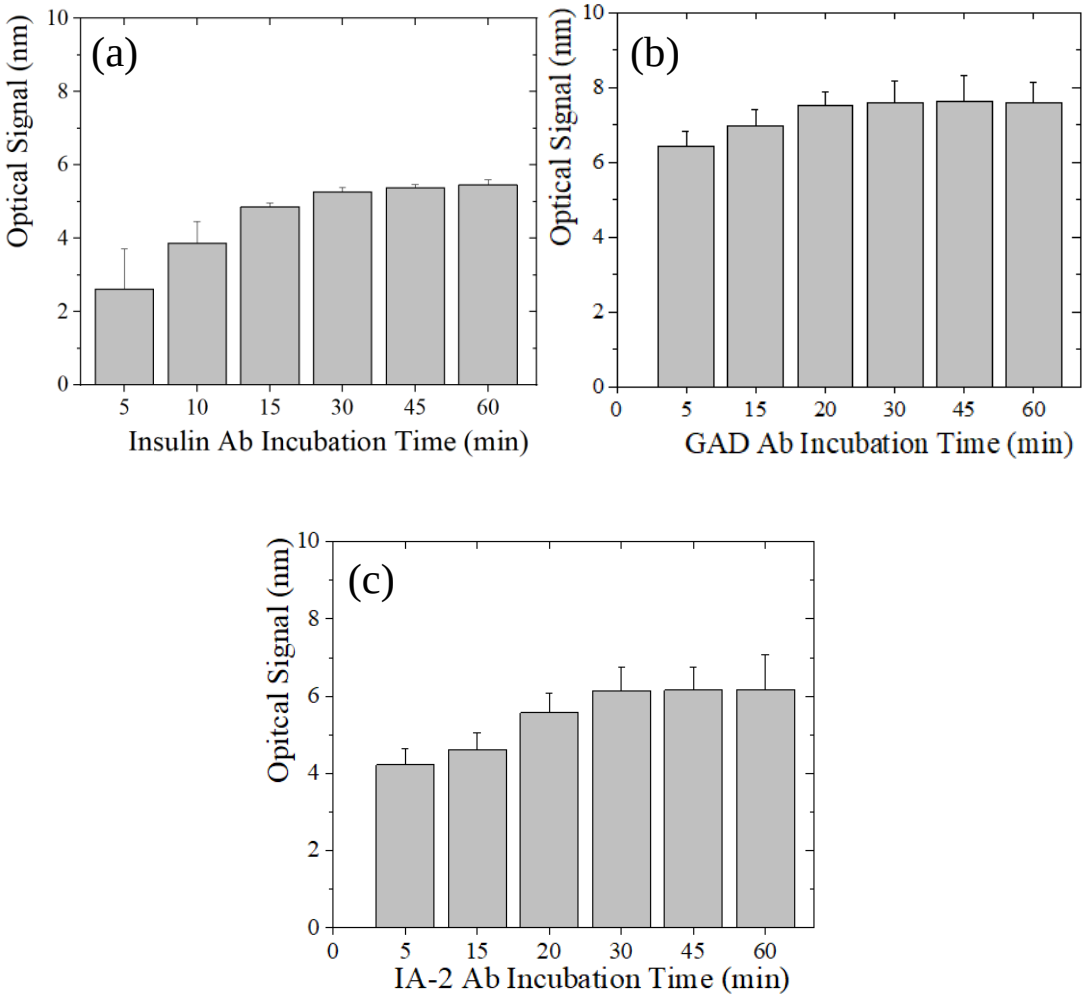

Fig 2. 5 (a) Insulin Ab saturation time around 30 to 45 mins (b) GAD Ab saturation time around 30 to 45 mins (c) IA-2 Ab saturation time around 30 to 45 mins

For the incubation time test, since the saturation time for antibody hostile to insulin, GAD, and IA-2 ranges from 30 mins to 45 mins, in the following standard test, the sample was incubated (shake) for 45 mins, allowing enough time to let antibodies bind with antigens. Currently, as little as 0.1 U/ml of three autoantibodies can be readily detected in both buffer solution and serum, while up to 50 U/ml of insulin Ab and GAD Ab and up to 100 U/ml of IA-2 Ab can be detected. As the antibody concentrations increased, the optical signal would increase. Results of the standard test for three antibodies are shown in **Fig 2.6**.

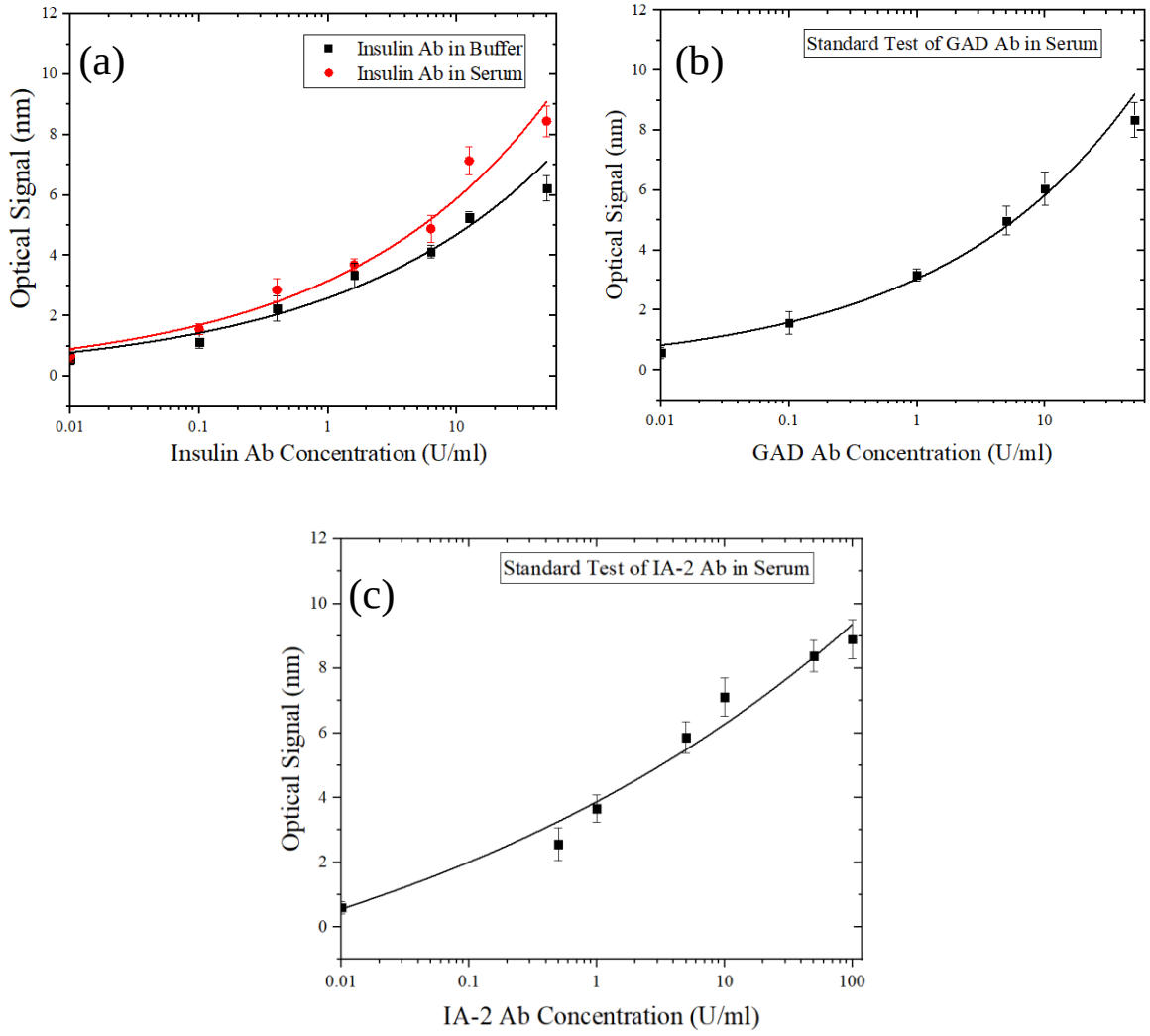

Fig 2. 6 (a) Standard test of Insulin antibody as concentration from 0.01 U/ml to 50 U/ml in both serum and buffer. (b) Standard test of GAD antibody from 0.01 U/ml to 50 U/ml only in serum. (c) Standard test of IA-2 antibody from 0.01 U/ml to 100 U/ml only in serum. Note that concentrations of the anti-insulin in buffer are known provide by vendor (adi Inc), as well as the concentration of antibodies against GAD, IA-2 in serum are known provided by Kronus.

Fig 2.6, the calibration curves with error bars indicate, optical signals occur when the concentration of antibodies increased, with a total of ~6 nm fringe shifts occurring in the insulin Ab test in the buffer along with a ~8.4 nm total shift in serum due to non-specific bindings in serum. Moreover, a total of ~ 8.2 nm and a total of ~9 nm fringes shift occurred in the GAD Ab, IA-2 Ab tests respectively, within the designated antibody concentration

range. For the anti-insulin sample, the lower detection limit is around 0.1 U/ml, and the detection limit of GAD antibody is also around 0.1 U/ml while the detection limit of anti-GAD ELISA is 0.2 U/ml [19]. The lower anti IA-2 ELISA (IgG) was found to be 0.7 U/ml [19], while in our test, IA-2 antibodies' detection limit is closed to 0.2 U/ml, more sensitive than available ELISA kit.

Based on standards provided by the vendors (adi Inc and Kronus), the normal range of insulin should be less than 5 U/ml, border-line is between 5 U/ml and 10 U/ml, and diabetes can be diagnosed if insulin concentration is larger than 10 U/ml. For the GAD and IA-2 antibodies, 5 U/ml is the threshold level, and once the concentration exceeds that value, diabetes can be confirmed.[20][21] Our optical sensor could easily detect the antibodies hostile to insulin, GAD, and IA-2 above the 5 U/ml level. To observe fringe shift in the samples, we could easily distinguish whether or not antibodies had bound with antigens. Overall, our sensor could successfully detect the autoantibodies against insulin, GAD, and IA-2 in the sample.

Results of the specificity test are indicated in **Fig 2.7**. Antibodies would theoretically not bind with the non-specific antigen e.g.; insulin antibodies would bind with neither GAD antigens nor IA-2 antigens. After incubating antibodies on non-specific antigens for a certain time, antibodies can be washed away and ideally cause no fringe shift. Although in reality, the fringes will exhibit a certain amount of shift in such case, possibly generated by unknown elements presence in the serum that could, causes some non-specific binding, producing different optical signals.

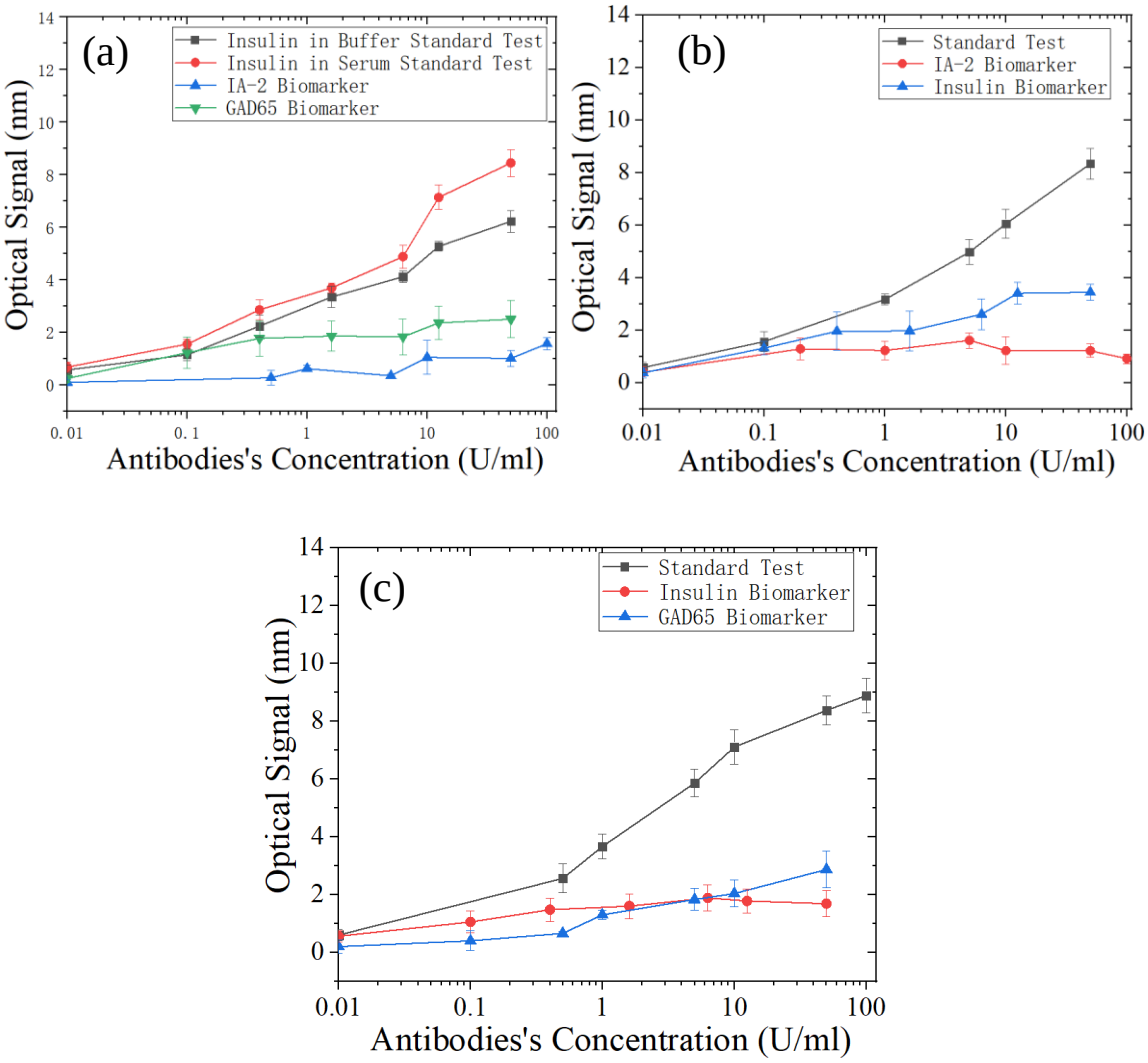

Fig 2. 7 (a) Specificity test of insulin antigens functionalized with three antibodies. (b) Specificity test of GAD antigen functionalized with three antibodies (c) Specificity test of IA-2 antigen functionalized with three antibodies.

As shown in **Fig 2.7 (a)**, insulin antigen-functionalized sensor indicated that insulin antibodies bind with insulin antigens to produce 6 nm fringe shift in buffer and 8.4 nm fringe shift in serum, while there was only an approximately 2.1 nm shift for GAD Ab and less than a 2 nm shift for IA-2 Ab in this case. **Fig 2.7 (b)** shows a shift of less than 2 nm for both IA-2 Ab and insulin Ab in a GAD Ag-functionalized sensor, much less than the shift for the GAD

Ab. An approximate 3 nm shift for GAD Ab and 2 nm shift for insulin Ab emerged on the IA-2 Ag functionalized sensor, as shown in **Fig 2.7 (c)**.

Fringe shifts occurring in the specificity test, were much smaller than those in the standard test, as low as 0.5 U/ml of each autoantibodies can be distinguished from a mixed-antibodies sample from **Fig 2.7,** reflecting good specificity of this label-free optical sensor.

Overall, the label-free sensor can successfully detect the autoantibodies against insulin, GAD, and IA-2, through observation of optical-signals shifts related to different antibody concentrations. While the non-specific binding caused by the unknown chemical composition in the antibody solvent (buffer or serum) will lead to a small amount of fringe shift, they do not challenge recognition of antibodies whether or not they are matches to antigens.

References

[1] Zimmet, P., Alberti, K. G., Magliano, D. J., & Bennett, P. H. (2016). Diabetes mellitus statistics on prevalence and mortality: facts and fallacies. *Nature Reviews Endocrinology*, *12*(10), 616.

[2] Yu, L., Robles, D. T., Abiru, N., Kaur, P., Rewers, M., Kelemen, K., & Eisenbarth, G. S. (2000). Early expression of antiinsulin autoantibodies of humans and the NOD mouse: evidence for early determination of subsequent diabetes. *Proceedings of the National Academy of Sciences*, *97*(4), 1701-1706.

[3] Turner, R., Stratton, I., Horton, V., Manley, S., Zimmet, P., Mackay, I. R., ... & UK Prospective Diabetes Study (UKPDS) Group. (1997). UKPDS 25: autoantibodies to islet-cell cytoplasm and glutamic acid decarboxylase for prediction of insulin requirement in type 2 diabetes. *The Lancet*, *350*(9087), 1288-1293.

[4] Atkinson, M. A., Eisenbarth, G. S., & Michels, A. W. (2014). Type 1 diabetes. *The Lancet*, *383*(9911), 69-82.

[5] Soltesz, G., Patterson, C. C., Dahlquist, G., & EURODIAB Study Group. (2007). Worldwide childhood type 1 diabetes incidence–what can we learn from epidemiology? *Pediatric diabetes*, *8*, 6-14.

[6] Delic-Sarac, M., Mutevelic, S., Karamehic, J., Subasic, D., Jukic, T., Coric, J., ... & Zunic, L. (2016). ELISA test for analyzing of incidence of type 1 diabetes autoantibodies (GAD and IA2) in children and adolescents. *Acta Informatica Medica*, *24*(1), 61.

[7] Tiberti, C., Yu, L., Lucantoni, F., Panimolle, F., Spagnuolo, I., Lenzi, A., ... & Dotta, F. (2011). Detection of four diabetes specific autoantibodies in a single radioimmunoassay: an innovative high-throughput approach for autoimmune diabetes screening. *Clinical & Experimental Immunology*, *166*(3), 317-324.

[8] Zhang, B., Kumar, R. B., Dai, H., & Feldman, B. J. (2014). A plasmonic chip for biomarker discovery and diagnosis of type 1 diabetes. *Nature medicine*, *20*(8), 948.

[9] Duan, K., Ghosh, G., & Lo, J. F. (2017). Optimizing Multiplexed Detections of Diabetes Antibodies via Quantitative Microfluidic Droplet Array. *Small*, *13*(46), 1702323.

[10] Zhang, T., He, Y., Wei, J., & Que, L. (2012). Nanostructured optical microchips for cancer biomarker detection. *Biosensors and Bioelectronics*, *38*(1), 382-388.

[11] Song, C., Deng, P., Ding, X., & Que, L. (2018). A Flexible Nanopore Thin-Film-Enabled Device for Pressure Sensing and Drug Release. *IEEE Transactions on Nanotechnology*, *17*(5), 962-967.

[12] Song, C., Ding, X., & Que, L. (2018). High-resolution, flexible, and transparent nanopore thin film sensor enabled by cascaded Fabry–Perot effect. *Optics letters*, *43*(13), 3057-3060.

[13] Song, C., Che, X., & Que, L. (2017). Nanopore thin film enabled optical platform for drug loading and release. *Optics express*, *25*(16), 19391-19397.

[14] Alzghoul, S., Hailat, M., Zivanovic, S., Que, L., & Shah, G. V. (2016). Measurement of serum prostate cancer markers using a nanopore thin film based optofluidic chip. *Biosensors and Bioelectronics*, *77*, 491-498.

[15] Feng, S., Chen, C., Wang, W., & Que, L. (2018). An aptamer nanopore-enabled microsensor for detection of theophylline. *Biosensors and Bioelectronics*, *105*, 36-41.

[16] Song, C., Deng, P., & Que, L. (2018). Rapid multiplexed detection of beta-amyloid and total-tau as biomarkers for Alzheimer's disease in cerebrospinal fluid. *Nanomedicine: Nanotechnology, Biology and Medicine*, *14*(6), 1845-1852.

[17] He, Y., Li, X., & Que, L. (2014). A transparent nanostructured optical biosensor. *Journal of biomedical nanotechnology*, *10*(5), 767-774.

[18] Zhang, T., Gong, Z., Giorno, R., & Que, L. (2010). A nanostructured Fabry-Perot interferometer. *Optics express*, *18*(19), 20282-20288.

[19]Delic-Sarac, M., Mutevelic, S., Karamehic, J., Subasic, D., Jukic, T., Coric, J., ... & Zunic, L. (2016). ELISA test for analyzing of incidence of type 1 diabetes autoantibodies (GAD and IA2) in children and adolescents. *Acta Informatica Medica*, *24*(1), 61.

[20] Alpha Diagnostic Intl. (n.d.). *For the Quantitative Determination of Autoantibodies to Insulin in human serum or plasma*. Manuscript submitted for publication. Retrieved January 15, 2019.

[21] KRONUS. (n.d.). Glutamic Acid Decarboxylase Antibody (GADAb). Retrieved March 14, 2019, from https://www.kronus.com/product_catalog/index.php

CHAPTER 3. FABRICATION OF LABEL-FREE OPTICAL SENSOR WITH MICROFLUIDICS INTERFACE

Abstract

Microfluidics is extensively used in many multidisciplinary fields, like engineering, physics, chemistry, biotechnology and nanotechnology that use such devices to apply fluid flow to channel in a small dimension, usually less than 1 millimeter. Microfluidics has a number of useful advantages, including reduce reagent consumption, applicable to well-controlled particle manipulation, and multiplexing screening. A microfluidic interface with the label-free optical sensor of this study can achieve multiplexed detection of autoantibodies against Type 1 Diabetes. There is a great need for quantitative detection of all three antibodies within a single volume, and the detailed fabrication process of the microfluidic surface for this purpose and the sensor's micropattern process will be discussed in this chapter.

3.1 Introduction

Manipulation of fluidics in channels at micro-scale or less, called microfluidics, has arisen as a unique field promising to influence multidiscipline from engineering, chemical, physics, and nanotechnology. The roots of microfluidics originated from three main different fields, microanalysis, biodefense, and microelectronics. It was first applied in 1970s [1] as a tool in microbiology by supporting operation of a small volume of sample and reagent in analysis to achieve a miniaturized gas chromatography on a silicon wafer. Still, another motivation for microfluidics resulted from chemical and biological weapon threats posed by the hostile parties, where microfluidics systems were designed in 1990s [2] to serve as

detectors for chemical biological threats, commissioned for fast and in-situ detection. Another contribution came from microelectronics in photolithography and related technologies used to form microfluidics devices using silicon or glass as raw materials. Although silicon was soon after replaced by polymer because of its low cost, high biocompatible, and transparency to UV light, a polymer is an elastomer, a more flexible material than rigid material silicon, with the important property of gas permeability, necessary for bio-detecting living cells in a microfluidic channel.

Over the years, materials such as silicon, glass, and polymers have been used to fabricate microfluidic devices, although admittedly there are no perfect materials; as all have both merits and defects when utilized in microfluidics. While silicon was one of the first materials used in microfluidics because of its good thermal conductivity and surface stability, the drawback of silicon is obvious; it is opaque to visible or UV light, so it cannot be used for high-resolution optical detection. Polymers are widely used in microfluidics fabrication due to advantages like, biocompatibility. In contrast, they might absorb small hydrophobic molecules. But, their future is still bright.

Most microfluidic systems have been implemented in polymer- polydimethylsiloxane (PDMS), a silicon-based organic polymer whose properties are somewhat different from silicon or glass. There are many reasons for PDMS becoming a popular material for fabricating microfluidic devices. It is transparent, and compatible the optical detection from 240 nm to 1100 nm [4]. It has good deformability that can be used in valve application through channel deformation. It is also permeable to gases, and biocompatible, important properties in experiments involving living cells, or supplying gas supplying for cell cultures. Additionally,

PDMS is cost-effective, cheaper than silicon or glass. Hence, we employ PDMS as material to fabricate the microfluidics interface for the label-free optical sensor. The motivations for using microfluidics are that they can be used to greatly reduce the sample usage and multiplexed detection of autoantibodies using in a single chip, with the PDMS an appropriate material for realizing bio-detection.

Soft lithography is a common technique used to fabricate PDMS structures. This process requires a mold to depicts the hollow space for the microfluidics channel. PDMS is a proportional mixture of silicon hydride groups and vinyl groups that can be poured on the top of a mold. Then Peeled off the PDMS from the mold after 2 hours curing at 75°C. The structure is ultimately transferred from the mold to a PDMS replica whose channel has no bottom. To form a closed channel, Plasma Bonding can be used to seal the PDMS to a surface, such as glass or silicon. As a result, a general microfluidic system is formed.

A micropatterned AAO is important for integrating the label-free optical sensor with the microfluidics structure. The micropattern process has been successfully accomplished on the glass substrate using an anodization (one-step or two-step) process along with a lift-off process [3]. The properties of the micropattern AAO were evaluated to verify that its optical properties remain unchanged. Therefore, suggesting that the down-sized optical sensor stored in a microfluidic channel can significantly reduce sample usage.

3.2 Materials and Fabrication process

1. Materials and chemicals

Silicon wafer is purchased from Wafer World, Inc. Negative photoresist SU-8 2075 and SU-8 developer are purchased from MicroChem, Inc. The positive photoresist AZ 5214-E IR and AZ 300 MIF developer are purchased from EMD Performance Materials Corp. PDMS is 184 silicone elastomers purchased from SYLGARD™. And Aluminum etchant Type A is purchased from TRANSENE, Inc. AAO etchant is a mixture of phosphoric acid (0.4M) and chromic acid (0.2M)

2. Micropattern AAO process

Device fabrication involves two aspects: fabrication of anodic aluminum oxide (AAO) nanopore thin film-based sensors and a PDMS microfluidic layer, and fabrication process flow for the micropattern AAO nanopore thin film sensor is shown in **Fig. 3.1**. Combining the anodization process of Al thin film with optical lithography, the fabrication process of the microfluidic interface is shown in **Fig. 3.3**.

The detailed fabrication process of the micropatterned anodic aluminum oxide sensor is shown in **Fig.3.1**. A 3″ x 1″ glass substrate is first washed thoroughly in four steps: DI water, acetone, IPA and more DI water in sequence. An approximately 10 nm thick titanium layer and a 2 μm thick aluminum layer are then deposited on the glass substrate by E-beam evaporation as shown in **Fig 3.1(b)**. The purpose of the titanium layer is to enhance adhesion between aluminum and glass. The anodization process (either one-step or two-step) uses 0.3 M of chromic acid ($H_2C_rO_4$) solution at 30V applied voltage at 5 °C for approximately 60 mins (one-step process), forming an approximate 1.2 μm to 1.4 μm thick AAO layer on the

glass substrate. Besides, for the two-step anodization process of forming AAO, the Al-coated glass substrate is placed into a chromic solution for about 20 minutes under the same conditions as in the one-step process, the sample is etched using 6wt.% phosphoric acid (H_3PO_4) at room temperature for 10 minutes, then, put back into the chromic solution for anodization process for another 40 minutes, forming an AAO thin film on the glass substrate. In this study, we used a one-step anodization process to form our AAO nanopore thin film.

To integrate the AAO sensor with the microfluidics device, we required a size reduction process, called Micropattern AAO. E-beam evaporation was first used to deposit a thin layer of aluminum on the AAO surface, followed by a spun a layer of photoresist AZ on which a photomask pattern of **Fig 3.2**, was created to selectively protect areas to be exposed to UV light. After UV exposure the glass substrate was immersed in AZ developer to remove exposed photoresist, as shown in **Fig 3.1(f)**. Once photoresist windows have been open, the unprotected Al was etched with aluminum etchant. Once the exposed Al was completely etched away, the glass substrate was immersed into AAO etchant to remove the unprotected AAO layer, as shown in **Fig 3.1(g)**. Finally, the photoresist layer was developed, and Al layer etched in sequence. revealing the AAO nanopore thin film sensor on the glass substrate indicated in **Fig 3.1 (h)**.

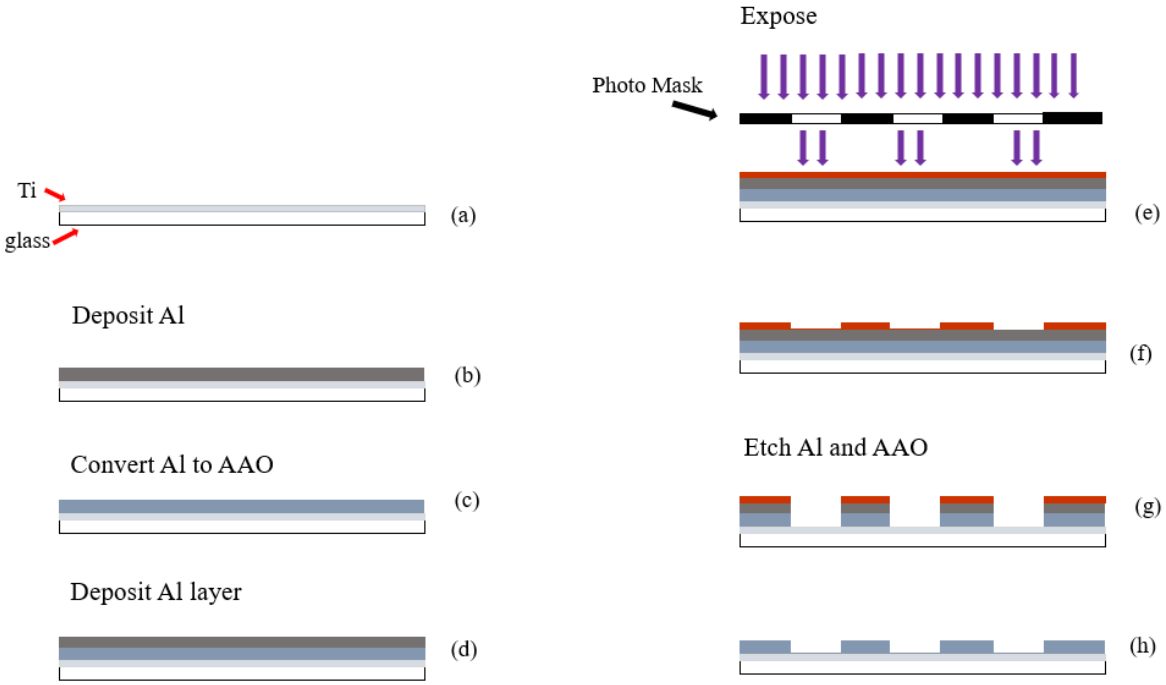

Fig 3. 1 Fabrication flow of micropattern AAO thin film sensor

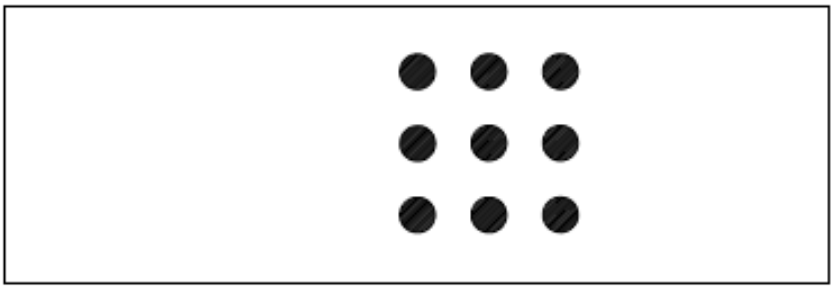

Fig 3. 2 Photomask of micropattern AAO nanopore thin film with the diameter of 3.5 mm

3. Microfluidic Device Fabrication Process

To fabricate the microfluidics interface for the optical sensor, a mold was designed using SketchUp then print on a transparent mask shown in **Fig. 3.3**.

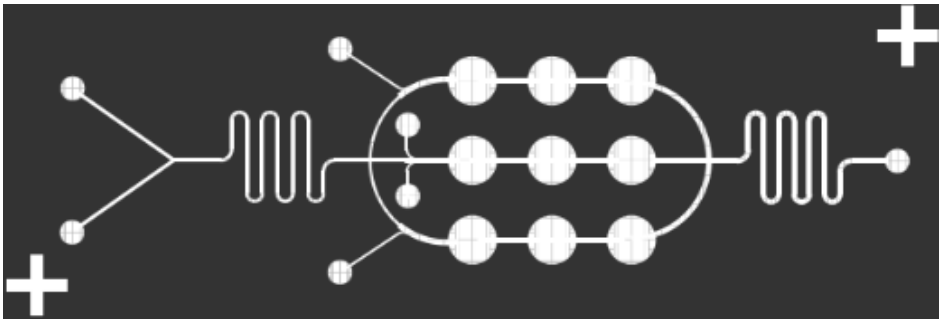

Fig 3. 3 SketchUp designed photomask for optical sensor.

This design consists of three rows of three sensors, each with a nanopore thin film layer. The sensors were located at the center of the white circular area of diameter 4 mm, and each sensor has a diameter of about 3.5 mm. The microfluidic channel has two different dimensions, as shown in **Fig 3.3**, with a 400 μm wide thick channel and 250 μm wide thin channel.

Photolithography was used to create mold using the fabrication process illustrated in **Fig. 3.4**. A 3″ silicon wafer was first cleaned with acetone and DI water, followed by pouring a pile of SU-8 on the wafer until it covered most of the wafer surface. The wafer was then spun on a spin coater at 2000 rpm for 30s, producing a 100 μm thickness, then soft-baked overnight at 45 °C. The designed photomask was then placed on the SU-8 coated wafer, followed by an UV exposure dose of 220 mJ/cm^2. Next, a hotplate set at 90°C provided a post-exposure bake directly after exposure, and once a clear view of the pattern emerged, the wafer was immersed in SU-8 developer to remove unexposed photoresist, while checking the pattern every 30s until only the microfluidics channel remained on the wafer. As a final step, the wafer was rinsed with DI water to remove residuals.

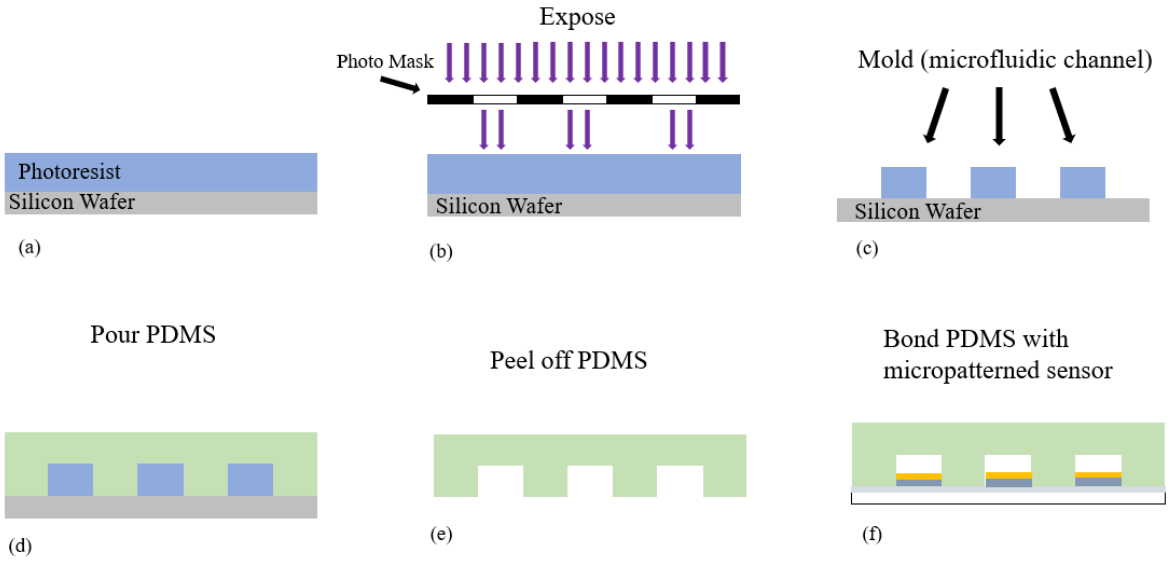

Fig 3. 4 Cross-section view of photolithographt and PDMS soft lithography process

Once the mold where the fluidic is to eventually flow has been formed on the wafer, as shown in **Fig 3.4(c)**, a PDMS mixture of silicone elastomer base and curing agent in a ratio of 1:9 was poured on the mold, followed by 2 hours of degassing and 2 hours of curing at 75°C. PDMS was then peeled off and the mold pattern transferred to the PDMS replica, then plasma bonded with the gold-coated patterned AAO sensor, as shown in **Fig 3.4(f)**.

3.3 Results and Discussion

1. Fabricated Device

The 3D sketch of the device is illustrated in **Fig 3.5**. Using the fabrication flow in **Fig 3.1** and **Fig 3.4**, the microfluidic devices have been fabricated. A photo of a fabricated device is illustrated in **Fig 3.6**. It has 9 sensors in three rows and each row has 3 identical sensors. The 3 sensors in each row are used to detect the same antibody. The measurement for one autoantibody is obtained by averaging the measurements from three sensors in the same row.

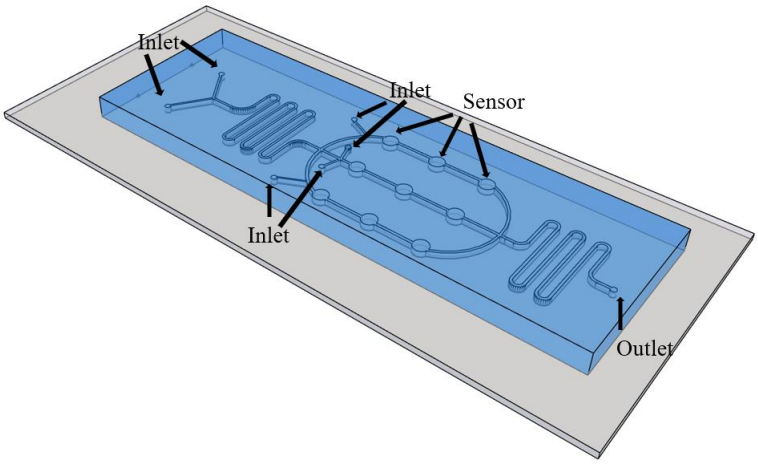

Fig 3. 5 Schematic of a device containing 3-row nanopore thin-film based sensors

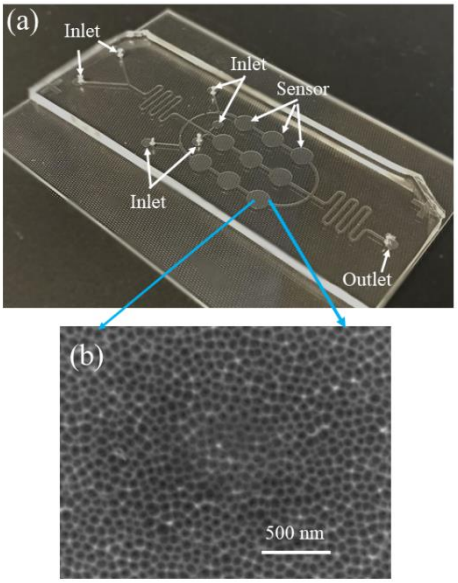

Fig 3. 6 (a) photo of a fabricated device containing 3-row nanopore thin-film based sensors; (b) SEM image showing the nanopores of the sensor.

2. Microfluidic Operation Demonstration

Three food dyes representing three different autoantibodies were used to demonstrate the functionality of the microfluidic network as shown in **Fig 3.7**. The surface functionalization process, shown in **Fig 2.2**, was carried out by flowing chemicals through

inlets. Specifically, *$HSC_{10}COOH/HSC_8OH$* and *NHS/EDC* flowed in Inlet 1 and Inlet 2, followed by three antigens introduced through Inlet 3, Inlet 4 and Inlet 5, respectively, loading the EA into entire sensor either through Inlet1 or Inlet 2. After these steps, surface functionalization of all sensors on this device has been accomplished.

Three autoantibodies could then be introduced through Inlet 3, Inlet 4 and Inlet 5. For the demonstration, three autoantibodies, mimicked by three food dyes (blue, red and green), could be simultaneously detected by the sensor on device.

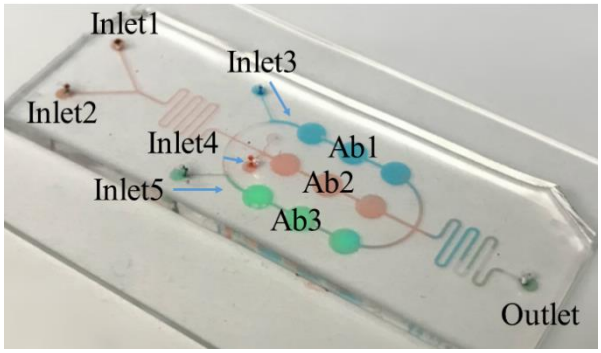

Fig 3. 7 Photo of the device: three food dyes (blue, red and green) to mimic three autoantibodies inside the chip showing its capability for multiplexed detection of three autoantibodies (insulin Ab, GAD Ab, and IA-2 Ab) by three sensors in three rows.

3. Measurements and Data Analysis

The measurements were carried out using a specifically designed optical fiber probe and a portable spectrometer (Ocean Optics, Inc.,) [5] the same optical equipment used in previous experiments. After autoantibodies were applied to the sensors and waiting approximately 30-50 for signals to become stable, and three-time rigorous rinse by PBS buffer were used to remove unbound autoantibodies on the sensor surface, after which,

results were obtained using three optical measurements. Furthermore, we also increased the concentrations of all three autoantibodies to be the same as those described in Chapter 2, then loaded them into sensors and obtained results by measuring their optical signals.

The test results were consistent with those generated by tests that directly applied samples onto the AAO thin film-based sensor. The total fringe shift of insulin in serum and the total fringe shift of insulin in buffer were ~8.7 nm and, ~6.3 nm respectively, compared with previous results of insulin, ~8.2 nm, ~6 nm in serum and in buffer. There were about 7.8 nm and 8.8 nm fringes shift for the GAD antibody and IA-2 antibody, while previous experiments had produced GAD Ab and IA-2 Ab signal shifts of ~8 nm and, ~9.2 nm, indicating a good consistency of results for both experiments. Overall, three autoantibodies against insulin, GAD, and IA-2 can be simultaneously detected by AAO thin film-based sensor integrated with microfluidic device.

References

[1] Terry, S. C., Jerman, J. H., & Angell, J. B. (1979). A gas chromatographic air analyzer fabricated on a silicon wafer. *IEEE transactions on electron devices*, *26*(12), 1880-1886.

[2] Tian, W. C., & Finehout, E. (2008). Microfluidic Applications in Biodefense. In *Microfluidics for Biological Applications* (pp. 323-384). Springer, Boston, MA.

[3] Yin, H., Li, X., & Que, L. (2014). Fabrication and characterization of aluminum oxide thin film micropatterns on the glass substrate. *Microelectronic Engineering*, *128*, 66-70.

[4] Whitesides, G. M. (2006). The origins and the future of microfluidics. *Nature*, *442*(7101), 368.

[5] S. Feng, C. Chen, W. Wang, L. Que, "An aptamer nanopore-enabled microsensor for detection of theophylline," *Biosensors and Bioelectronics, 105*, pp: 36-41, 2018

CHAPTER 4. CONCLUSION

In this thesis, the label-free optical sensor multiplexed detection of autoantibodies for Type 1 Diabetes has been reported. Autoantibodies against insulin, glutamic acid decarboxylase (GAD), and insulinoma associated protein-2 (IA-2) have been well-established in T1D panels and detecting the levels of such antibodies in samples is of a great interest, resulting in many approaches have been proposed for this purpose. Herein, anodic aluminum oxide nanopore thin-film based sensor integrated with microfluidic interface has been introduced to detect the autoantibodies in both a sample buffer and in serum. The AAO nanopore can be regarded as having in its cavity a nanostructured Fabry-Perot interferometer, a reactive-index sensitive optical sensor. We surface-functionalized the sensor with antigens, then applied the corresponding antibodies, and the transducing signal of the Fabry-Perot interferometer varied with the change of the effective refractive index in its cavity once the antibodies had bonded with the antigens. Different concentration of antibodies would result in distinct refractive index changes to yield different optical signals, and by observing optical signals shift, we can detect whether or not the sample contains autoantibodies. The specificity of the sensors was also evaluated, and a good specificity was indicated. The AAO nanopore thin-film based sensor was also integrated with microfluidic system, and it exhibited capability for simultaneously detection of all three autoantibodies.

By taking advantages of both anodic aluminum oxide thin film and microfluidics, we have made a contribution to detecting Type 1 Diabetes, and the demonstrated multiplexed detection is particularly important for providing predictive and screening values.

APPENDIX A. ANODIC ALUMINUM OXIDE FORMATION MECHANISM

Anodizing is an electrochemical process for converting metal surface into a corrosion resistant, anodic oxide finish. During the anodization process, the metal surface will grow an anodic oxide layer. For Aluminum, this process causes a porous oxide structure called anodic aluminum oxide (AAO) is formed on the Al surface.

The fabrication of AAO can be performed in the laboratory using the equipment shown in **Fig. A1**. The entire anodization process takes place in a reaction container filled with acid solution, with an associated cooling system connected to the tank to keeps flowing the water with the temperature at 2°C to 8°C to maintain the reaction temperature. The acid solution such as chromic acid, oxalic acid, phosphoric acid, or sulfuric acid is used as the electrolyte. Two electrodes, aluminum (Al) as the anode and platinum (Pt) as the cathode, are connected to a DC power supply that applies DC voltage between the two electrodes, causing the aluminum to gradually convert into anodic aluminum oxide. During this process, a stirring bar and magnetic stirrer are employed to maintain concentration uniformity in the acid solution.

Generally, the anodic aluminum oxide formation can be described using the equation $Al + acid + voltage \rightarrow nanopores$. The nanopore size is determined by the type of acid solution and amount of applied voltage. AAO formation is accomplished in two stages. In the first stage, a constant current density is maintained, while the voltage increases, and to maintain the current density, a barrier layer grows to maintain constant electric field strength. In the second stage, the barrier layer grows by a combination of migration of Al^{3+} ions outwards into the electrolyte and inward motion of O^{2-} and OH^- ions. The O^{2-} and OH^- ions

combine with Al to form oxide as shown in **Fig. A2(a)**. During the oxide formation process, the barrier is constantly regenerated with further oxide growth, transforming into a semi-spherical oxide layer of constant thickness that forms the pore bottom, as shown in **Fig. A2(b)**. The overall reaction can be summarized by the following equations.

Porous oxide layer formation process, Al dissolve in electrolyte

$$2Al \rightarrow 2Al^{3+} + 6e^{-}$$

Chemical reaction at the cathode which produces hydrogen gas

$$6H^{+} + 6e^{-} \rightarrow 3H_2$$

Oxygen anions react with Al at metal/oxide boundary

$$2Al + 3O^{2-} \rightarrow Al_2O_3 + 6e^{-}$$

Al cations react with water molecules at oxide/electrolyte boundary

$$2Al^{3+} + 3H_2O \rightarrow Al_2O_3 + 6H^{+}$$

Overall reaction at electrode

$$2Al + 3H_2O \rightarrow Al_2O_3 + 3H_2$$

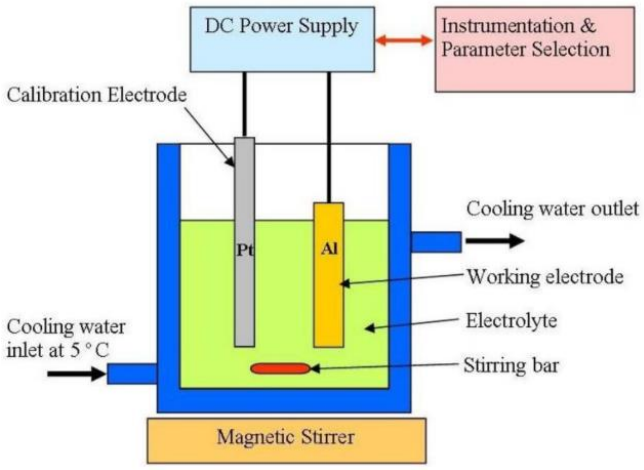

Fig A. 1 Experimental Equipment for producing anodic aluminum oxide [1]

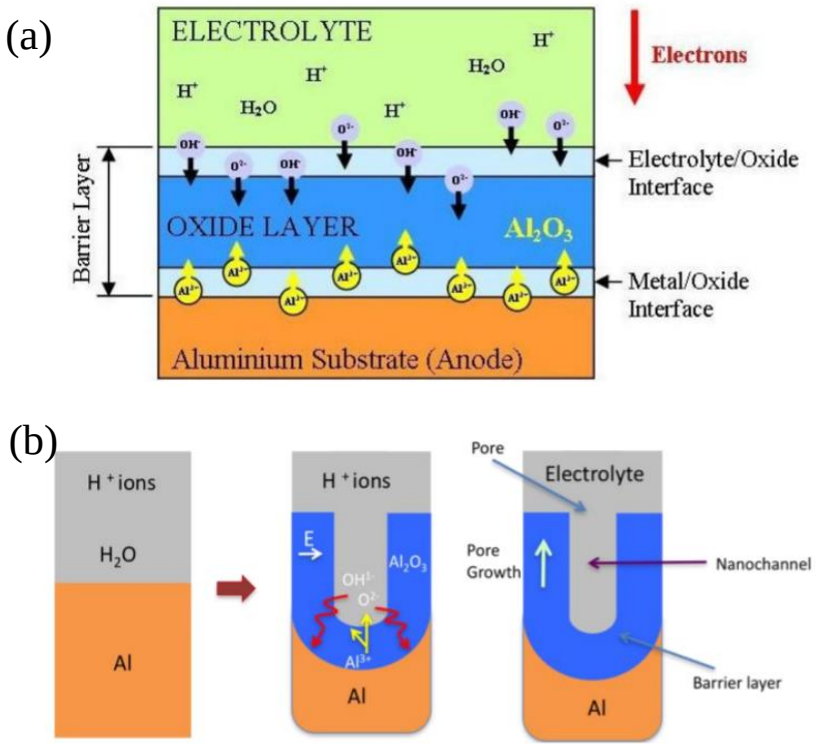

Fig A. 2 (a) Schematic of the major features involved in the formation of the barrier layer. (b) Schematic of pore formation mechanism in an acidic electrolyte [1]

Appendix A is summarized of journal paper, *Progress in nano-engineered anodic aluminum oxide membrane development.*

Reference

[1] Poinern, G. E. J., Ali, N., & Fawcett, D. (2011). Progress in nano-engineered anodic aluminum oxide membrane development. *Materials*, *4*(3), 487-526.

APPENDIX B. SURFACE FUNCTIONALIZATION MATERIALS AND PROTOCOL

Material

$HSC_{10}COOH/HSC_8OH$ (To form chemical bond on gold surface)

- 0.1mM 11-Mecaptoundecanoic acid (*$HSC_{10}COOH$*) and 0.9 Mm 8-Mercapto-1-Octanol (*HSC_8OH*)

NHS/EDC (activating reagent)

- 0.2 M N-hydroxy succinimide (NHS) and 005 M N-(3-dimethylamnopropyl)-N-ethyl carbodiimide hydrochloride (EDC) in DI H_2O

1 M *ethanolamine* (EA) dissolved in DI H_2O (To occupy the non-bonding spot)

Autoantibodies against insulin, GAD, and IA-2 dissolved in buffer and serum

- Insulin antibody is from Human Anti-Insulin IgG ELISA Kit, purchased from Alpha Diagnostic International Inc.

  Measuring the insulin antibody and dilute in both buffer and serum to yield the antibodies at concentration of 0.1 U/ml, 0.4 U/ml, 1.6 U/ml, 6.3 U/ml, 12.5 U/ml, 50 U/ml

- Glutamic Acid Decarboxylase antibody is purchased from vendor (Kronus. Inc.)

  Dilute the GAD Antibody into serum to get concentration at 0.1 U/ml, 0.5 U/ml, 1 U/ml, 5 U/ml, 10 U/ml, and 50 U/ml.

- Insulinoma associated Protein-2 is purchased from vendor (Kronus. Inc.).

  Dilute IA-2 Antibody into serum to get concentration at 0.5 U/ml, 1 U/ml, 5 U/ml, 10 U/ml, 50 U/ml and 100 U/ml

Protocol

In order to promote the surface functionalization process, a thin gold layer is sputtered on the anodic aluminum oxide surface to enhance the optical properties of the sensor. The transducing signals from the gold coated sensor is much apparent than the signal directly obtaining from the AAO thin film. The surface functionalization procedure is illustrated in **Fig. 2.2**. The step by step surface functionalization process is described below.

i. Prepare the Au coated AAO slides, rinse it with deionized water, acetone, Isopropyl alcohol (IPA) and deionized water one by one for three times. Dry out the AAO slides. And record the initial fringes.

ii. Using pipet to load enough $HSC_{10}COOH/HSC_8OH$ solution to cover AAO surface and incubate it at 4 ℃ overnight.

iii. Rinse the AAO slides thoroughly with ethanol and DI water for three times. Dry out and record the fringes.

iv. Apply *NHS/EDC* solution to cover AAO slides at room temperature for 2 hours.

v. Rinse the AAO slides with phosphate buffered saline (PBS) and DI water three times and dry out.

vi. Apply the antigens onto the AAO surface at 4 ℃ overnight.

Recommend antigens concentration:

Insulin antigen: 0.1 mg/ml

GAD antigen: 3 μmol/L

IA-2 antigen: 3 μmol/L

vii. Rinse the AAO slides with PBS and DI water thoroughly for three times, dry out and record the fringes.

viii. Apply EA solution onto AAO surface at room temperature for 2 hours.

ix. Rinse the AAO slides with PBS and DI water for 3 times, dry out and record fringes.

After above steps finished, the surface has been functionalized with the specific antigen, and it is ready to facilitate the either incubation time test or standard test.

APPENDIX C.THE OPERATIONAL PRINCIPLE OF ANODIC ALUMINUM OXIDE

The label-free optical sensor is anodic aluminum oxide thin film based which is a honeycomblike nanostructure. Inside the structures' cavity, it's a nanostructured Fabry-Perot interferometer (FPI) coated with a layer of gold. For the label-free biosensing, there are three main transducing mechanisms, which include electrical, mechanical and optical response. Electrical transduction is realized where the electrical conductance varies upon the binding between receptors and targets. Mechanical transduction is achieved by the binding between receptors and targets, resulting in its bending and resonant frequency shift due to the surface stress variance. In addition, FPI is a refractive-index sensitive sensor, the transducing signal will shift as the surface properties varying.[1]

As mentioned in surface functionalization process, we functionalize the AAO thin film surface with the chemicals, antigens, and antibodies. These processes could change the nanostructured surface properties. Immobilization of antibody receptors on the nanostructure layer and its binding with antibodies inside FPI are monitored in real time, resulting in transducing signal shift.

The **Fig.C1** indicates the nanostructured FPI sensor. The AAO sensor is integrated with the microfluidic interface. FPI cavity is serving as the biosensing area, the gold layer is coated on the surface of the nanopore which is to amplified transducing signals. The optical fiber emits the light signals and gets the reflected signal from FPI. Specifically, after the receptor (Ag) is attached on the sidewall of the nanopores, we can get the reflected signal from the sensor called S1. After antibody binding with the receptor (Ag), we can get another reflected signal from the sensor, called S2. The difference between S1 and S2 is $\Delta\lambda$ which is

the fringes shift occurred between two conditions since it's a refractive-index sensitive optical sensor, the transducing signal of a Fabry-Perot interferometer varies on the changes of the effective.

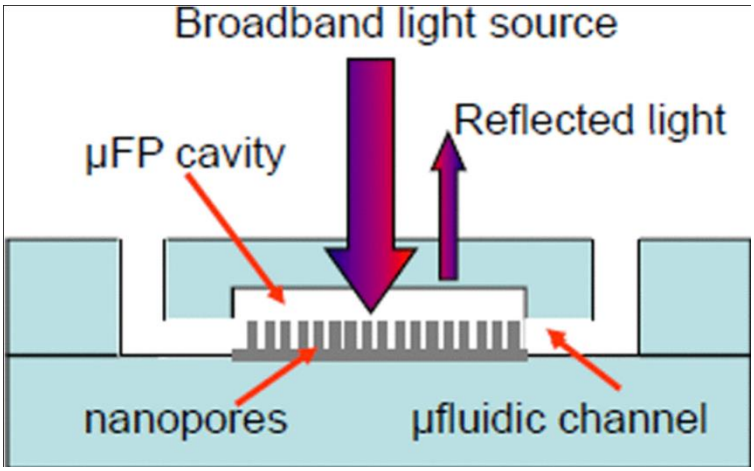

Fig C. 1 Schematic of the label-free nanostructured uFPI biosensor: Au-coated nanostructures are embedded in the FPI cavity [2][3]

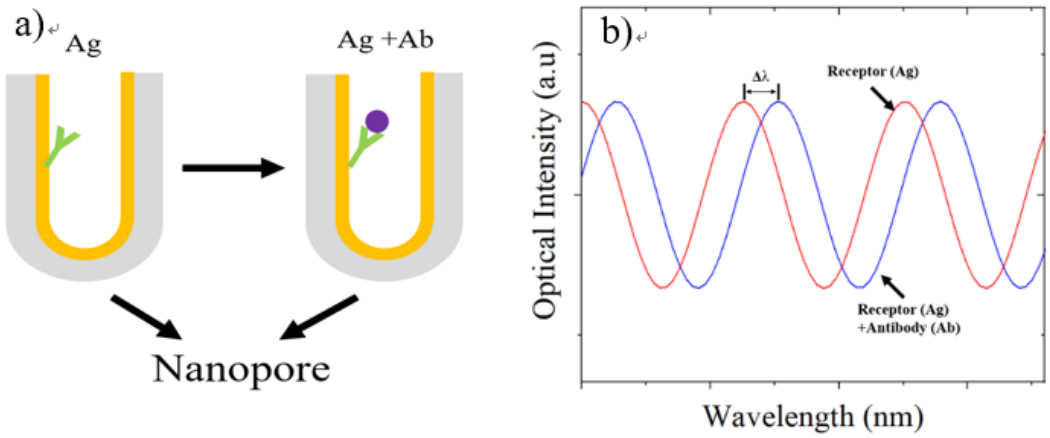

Fig C. 2 (a) Immoblization of antigen on the side wall of the nanopore, and after binding with antibody. (b) fringes indicate the signal produced from receptor only and after binding with antibody, fringes shift **Δλ** on the change of the effective refractive index.

References

[1] Zhang, T., Gong, Z., Giorno, R., & Que, L. (2010). A nanostructured Fabry-Perot interferometer. *Optics express*, *18*(19), 20282-20288.

[2] Zhang, T., Karandikar, S., Gong, Z., Giorno, R., & Que, L. (2010, November). Label-free biosensing using a nanostructured Fabry-Perot interferometer. In *SENSORS, 2010 IEEE* (pp. 2065-2068). IEEE.

[3] Zhang, T., Pathak, P., Karandikar, S., Giorno, R., & Que, L. (2011). A polymer nanostructured Fabry–Perot interferometer based biosensor. *Biosensors and Bioelectronics*, *30*(1), 128